

Quantitative Comparison of Color Performances Between IPS and MVA LCDs

Ruibo Lu, Qi Hong, Shin-Tson Wu, Kuo-Hsuan Peng, and Hung-Sheng Hsieh

Abstract—Color gamut and color shifts of the film-compensated multi-domain in-plane-switching (IPS) and multi-domain vertical alignment (MVA) liquid crystal displays (LCDs) are calculated quantitatively using light-emitting diodes (LEDs) and cold-cathode fluorescent lamp (CCFL) backlight. Simulation results indicate that the LED backlight exhibits better angular color uniformity and smaller color shifts than CCFL. In addition, the color gamut can be further widened and the color shift reduced when using color-sequential RGB-LED backlight without color filters. In general, both IPS and MVA LCDs show relatively small color shift under different backlights, but MVA has a lower color shift using the optimized uniaxial compensation films.

Index Terms—Backlight, color, color shift, in-plane switching (IPS), light-emitting diode (LED), liquid crystal display (LCD), multi-domain vertical alignment (MVA).

I. INTRODUCTION

LIQUID crystal displays (LCDs) using a light-emitting diode backlight unit (LED BLU) offer tremendous performance advantages over the conventional cold-cathode fluorescent lamp (CCFL) in larger color gamut, higher brightness, tunable backlight white point control by separate red, green and blue (RGB) colors, real-time color management, reduced motion artifacts without brightness and lifetime penalty, and higher dimming ratio [1]–[4]. For high-end LCD monitors and TVs, small color shift, fast response time, wide viewing angle, high contrast ratio, and high optical efficiency are the major technical challenges [5]. To achieve these goals, the film-compensated multi-domain in-plane-switching (IPS) and multi-domain vertical alignment (MVA) LCDs are the two major approaches [6]–[8]. These LCDs exhibit wide viewing angle and high contrast ratio, however, color shift remains an important issue.

To reduce color shift and widen color gamut, LED backlights have been considered. However, only few quantitative results on the color performance of LCDs using LED backlights have been reported. In this paper, we calculate the color gamut and color shift of the film-compensated four-domain IPS and four-domain VA LCDs using LED and CCFL backlight units. In this case, conventional color filters (CFs) are still employed. In the second

case, we consider color-sequential LCDs using RGB LED backlights without color filters.

II. MODELING OF COLOR SHIFT

In the history of color science, several approaches and models have been developed to analyze the displayed color images [9]–[13]. Among them, the tristimulus method which is established and developed by the Commission International de l'Éclairage (CIE) [12] is a three-valued system. It can effectively model the appearance of color by human eye, including the specifications of the observer, light source, device, and other aspects of the viewing conditions. For the convenience of discussion, in the following sections we only briefly review the terminologies and definitions that are directly relevant to the LCD color performances.

A. Tristimulus Values and Chromaticity Coordinates for CIE 1931

The CIE XYZ color space defines all the colors in terms of three imaginary primaries X , Y , Z , and Z based on the human visual system. The X , Y , Z tristimulus values of a color stimulus ($S(\lambda)$) which represent the luminance or lightness of the colors are expressed as

$$\begin{aligned} X &= k \int_{380 \text{ nm}}^{780 \text{ nm}} S(\lambda) \bar{x}(\lambda) d\lambda \\ Y &= k \int_{380 \text{ nm}}^{780 \text{ nm}} S(\lambda) \bar{y}(\lambda) d\lambda \\ Z &= k \int_{380 \text{ nm}}^{780 \text{ nm}} S(\lambda) \bar{z}(\lambda) d\lambda. \end{aligned} \quad (1)$$

Here, the values of $\bar{x}(\lambda)$, $\bar{y}(\lambda)$, and $\bar{z}(\lambda)$ color matching functions are the tristimulus values of the monochromatic stimuli, $S(\lambda)$ represents the spectral radiometric quantity at a certain wavelength λ , e.g., it is the light transmission intensity in a practical LCD device, and k is a constant [12].

Since the X , Y , and Z tristimulus values are not easy to interpret so that it is difficult to tell what the color they specify, the chromaticity coordinates x , y , z have been introduced by CIE in the following forms:

$$x = \frac{X}{X+Y+Z}, \quad y = \frac{Y}{X+Y+Z}, \quad z = \frac{Z}{X+Y+Z} \quad (2)$$

Because $x + y + z = 1$, it is sufficient to just use two chromaticity coordinates to describe the chromaticity of the stimulus. That means x and y can be plotted in a two-dimensional graph containing all the color information of the original X , Y , and Z values. The corresponding chromaticity diagram

Manuscript received August 16, 2006; revised September 8, 2006. This work was supported by the Chi-Mei Optoelectronics Corporation, Tainan, Taiwan, R.O.C.

R. Lu, Q. Hong, and S.-T. Wu are with the College of Optics and Photonics, University of Central Florida, Orlando, FL 32816 USA (e-mail: rlu@mail.ucf.edu).

K.-H. Peng and H.-S. Hsieh are with the Technology Development Division, Chi-Mei Optoelectronics Corporation, Tainan Science-Based Industrial Park, Tainan 74147, Taiwan, R.O.C.

Color version of Figs. 2, 3(c), and 4–7 are available online at <http://ieeexplore.ieee.org>.

Digital Object Identifier 10.1109/JDT.2006.885158

is referred as CIE 1931 diagram which is the first standard colorimetric system including the color matching functions for the standard observer, standard illuminants, and standard light sources [13].

B. CIE 1976 Uniform Chromaticity Scale (UCS) Diagram

To obtain the reasonably equidistant chromaticity scales that are better than the CIE 1931 diagram, the CIE 1976 uniform chromaticity scale (UCS) diagram which is also called (u', v') diagram has been introduced. The (u', v') coordinates are related to the (x, y) coordinates by the following equations:

$$\begin{aligned} u' &= \frac{4X}{X + 15Y + 3Z} = \frac{4x}{-2x + 12y + 3} \\ v' &= \frac{9Y}{X + 15Y + 3Z} = \frac{9y}{-2x + 12y + 3} \end{aligned} \quad (3)$$

C. Color Shift Based on CIE Color Difference Equations

Color shift is an important parameter to determine the color uniformity of an LCD panel. The angular-dependent color uniformity of an LCD panel is usually measured by a spectro-radiometer with capacity of presenting u' and v' coordinates when the display color is set at the full-bright state. The chromaticity coordinates u' and v' are measured in the visually most color deviating areas such as the horizontal and vertical directions of an LCD panel.

Based on (3), $\Delta u'v'$ at any two positions (1 and 2) can be calculated using the following formula:

$$\Delta u'v' = \sqrt{(u'_2 - u'_1)^2 + (v'_2 - v'_1)^2}. \quad (4)$$

To characterize the color shift in a LCD monitor or TV, $[u'_2, v'_2]$ represent the $[u', v']$ values at an oblique viewing angle while $[u'_1, v'_1]$ are usually referred to the $[u', v']$ values at normal viewing angle.

In the following sections, we will evaluate the color shift of the film-compensated multi-domain IPS and MVA LCDs using RGB-LED and CCFL backlight units. The color shift is referred to the full-bright state, i.e., the 255th gray level (G255), of the corresponding LCD.

III. DEVICE STRUCTURES AND SIMULATION METHODS

A. Device Structures and Simulation Parameters

Fig. 1 shows the typical device structures of the simulated multi-domain IPS and MVA LCDs. For the IPS mode [see Fig. 1(a)], the chevron-shaped structure represents the inter-digital electrodes which are alternatively arranged on the same substrate as the common electrode and the pixel electrode, respectively. The LC directors are initially homogeneously aligned along the perpendicular direction on the glass substrates. The chevron-shaped electrode has a bending angle α which is set as the angle between the chevron arm extension direction and the vertical direction [14]. For the MVA mode [Fig. 1(b)], the chevron-shaped structure represents the slits which are alternatively etched on the bottom common electrode and the top pixel electrode. The LC directors are vertically aligned on the glass substrates in the initial state [15]. Here, the bending angle α refers to the angle between the slit arm

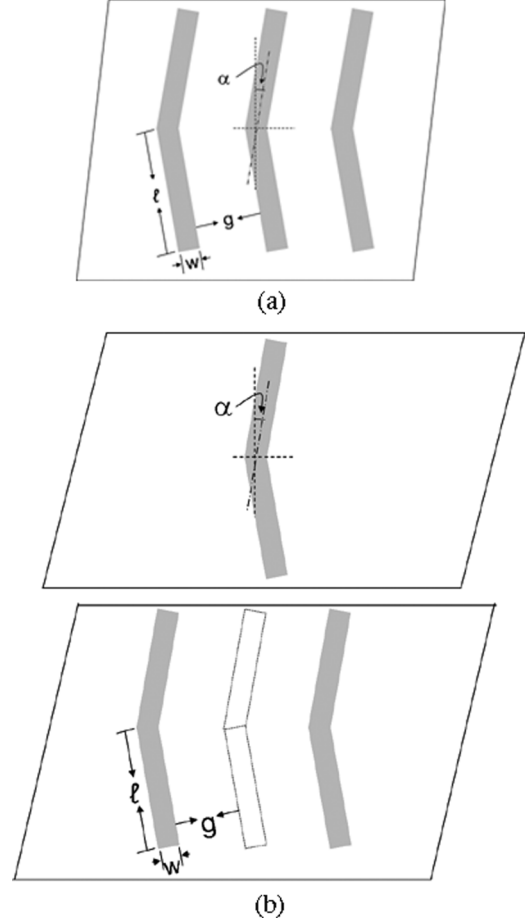


Fig. 1. Typical electrode structures of the multi-domain: (a) IPS and (b) MVA LCDs.

extension direction and the perpendicular direction. Both IPS and MVA LCDs work in the normally black mode between crossed linear polarizers, and both modes can realize 4-domain LC alignment configuration in the voltage-on state.

As an example, we simulate a chevron-shaped four-domain IPS LCD using a Merck positive LC material MLC-6692 and the MVA LCD using a Merck negative LC material MLC-6608. The physical properties of MLC-6692 are listed as follows: $\gamma_1 = 0.1 \text{ Pa} \cdot \text{s}$, $\Delta\epsilon = 10.3$, $K_{11} = 9.6 \text{ pN}$, $K_{22} = 6.1 \text{ pN}$, $K_{33} = 14.1 \text{ pN}$, and $\Delta n = 0.085$ at $\lambda = 550 \text{ nm}$, and for MLC-6608: $\gamma_1 = 0.186 \text{ Pa} \cdot \text{s}$, $\Delta\epsilon = -4.2$, $K_{11} = 16.7 \text{ pN}$, $K_{22} = 7.0 \text{ pN}$, $K_{33} = 18.1 \text{ pN}$, and $\Delta n = 0.083$ at $\lambda = 550 \text{ nm}$. The birefringence dispersion of the LC material at each wavelength of the light source is included in the calculation using the following equation [16]:

$$\Delta n = G \cdot \frac{\lambda^2 \cdot \lambda^{*2}}{\lambda^2 - \lambda^{*2}}. \quad (5)$$

At room temperature, the two fitting parameters are: $G = 1.6464 \times 10^{-6} \text{ nm}^{-2}$ and $\lambda^* = 210 \text{ nm}$ for MLC-6692, and $G = 1.6077 \times 10^{-6} \text{ nm}^{-2}$ and $\lambda^* = 210 \text{ nm}$ for MLC-6608.

In our design, the cell gap of the IPS LCD is $d = 4 \mu\text{m}$, the width of the chevron-shaped electrode is $w = 3 \mu\text{m}$, the electrode gap is $g = 8 \mu\text{m}$, and the chevron arm length is $l =$

128 μm . The bending angle of the chevron-shaped electrodes is typically chosen at $\alpha = 10^\circ$, and LC pretilt angle is 2° with respect to the substrate plane. For the MVA mode, the cell gap is $d = 4 \mu\text{m}$, the width of the chevron-shaped slit is $w = 6 \mu\text{m}$, the gap between the neighboring slits on the bottom and top substrates is $g = 18 \mu\text{m}$ on the projected plane, and the chevron arm length is $\ell = 62 \mu\text{m}$. The bending angle is at $\alpha = 45^\circ$, and LC pretilt angle is 90° with respect to the substrate surface.

In the practical IPS and MVA LCDs, compensation films are commonly used to widen the viewing angles of the devices [17]. For IPS LCD, a pair of positive A- and C-plates is added before the analyzer to widen the viewing angle, where the positive A-plate has $\Delta n \cdot d = 155.4 \text{ nm}$ with $n_e = 1.5124$ and $n_o = 1.5089$ at $\lambda = 550 \text{ nm}$, and the positive C-plate has $\Delta n \cdot d = 91.8 \text{ nm}$ with $n_e = 1.5124$ and $n_o = 1.5089$ at $\lambda = 550 \text{ nm}$ [14]. For MVA LCD, two sets of uniaxial films, a positive A-plate and a negative C-plate, are placed after the polarizer and before the analyzer, respectively. The film's $d\Delta n$ value is 93.2 and -85.7 nm , respectively. The positive A-plate has a $n_e = 1.5124$ and $n_o = 1.5089$ at $\lambda = 550 \text{ nm}$, and the negative C-plate has $n_e = 1.5089$ and $n_o = 1.5124$ at $\lambda = 550 \text{ nm}$ [18], [19]. During simulations, we assume the phase-matched compensation films have the same color dispersion as that of the LC material employed [20].

B. Simulation Approaches and Optical Calculations

The simulation sequence is to obtain the dynamic 3-D LC director distributions first and then calculate the detailed electro-optics of the LCD. We used a 3-D simulator to calculate the LC director distributions, which combines the finite element method and finite difference method approaches to improve the calculation speed [14].

Once the LC director distribution profiles are obtained, we then calculate the electro-optic properties of the LCD using the extended Jones matrix method [21]. The LC layer is modeled as a stack of uniaxial homogeneous layers. Here, we assume the reflections between the interfaces are negligible. Therefore, the transmitted electric field is related to the incident electric field by

$$\begin{bmatrix} E_x \\ E_y \end{bmatrix}_{N+1} = \mathbf{J} \begin{bmatrix} E_x \\ E_y \end{bmatrix}_1 = \mathbf{J}_{Ext} \mathbf{J}_N \mathbf{J}_{N-1} \cdots \mathbf{J}_2 \mathbf{J}_1 \mathbf{J}_{Ent} \begin{bmatrix} E_x \\ E_y \end{bmatrix}_1 \quad (6)$$

where \mathbf{J}_{Ext} and \mathbf{J}_{Ent} are the correction matrices considering the transmission losses in the air-LCD interface, which are given by

$$\mathbf{J}_{Ent} = \begin{bmatrix} \frac{2 \cos \theta_p}{\cos \theta_p + n_p \cos \theta_k} & 0 \\ 0 & \frac{2 \cos \theta_k}{\cos \theta_k + n_p \cos \theta_p} \end{bmatrix} \quad (7a)$$

$$\mathbf{J}_{Ext} = \begin{bmatrix} \frac{2n_p \cos \theta_k}{\cos \theta_p + n_p \cos \theta_k} & 0 \\ 0 & \frac{2n_p \cos \theta_p}{\cos \theta_k + n_p \cos \theta_p} \end{bmatrix}. \quad (7b)$$

Correspondingly, the overall optical transmittance is represented as

$$t_{op} = \frac{|E_{x,N+1}|^2 + \cos^2(\theta_p)|E_{y,N+1}|^2}{|E_{x,1}|^2 + \cos^2(\theta_p)|E_{y,1}|^2} \quad (8)$$

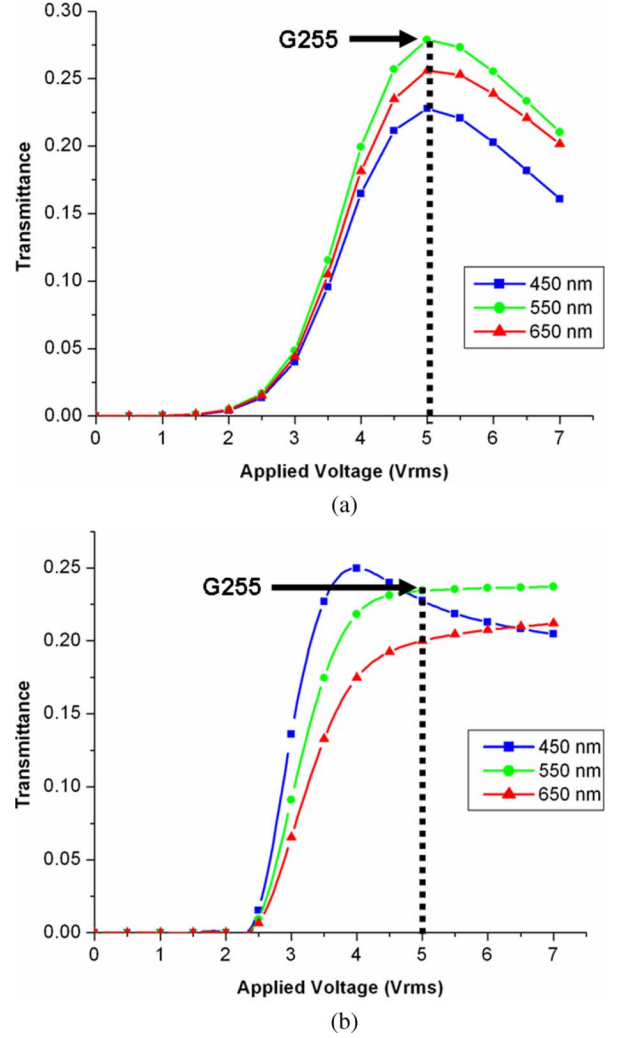


Fig. 2. The simulated VT curves of the multi-domain (a) IPS and (b) MVA LCDs at $R = 650$, $G = 550$, and $B = 450 \text{ nm}$.

where θ_p is given by

$$\theta_p = \sin^{-1}(\sin(\theta_k)/\text{Re}(n_p)). \quad (9)$$

Here, n_p is the average refractive index of the polarizer, where $n_p = (2n_{e,p} + n_{o,p})/3$, $n_{e,p} = 1.500 + i \times 3.251 \times 10^{-3}$ and $n_{o,p} = 1.500 + i \times 2.86 \times 10^{-5}$; $\text{Re}(n_p)$ stands for the real part of n_p ; θ_k is the azimuthal angle of the incident wavevector \mathbf{k} .

IV. RESULTS AND DISCUSSION

A. Voltage-Dependent Transmittance Curves

Fig. 2 shows the voltage-dependent transmittance (VT) curve of the multi-domain IPS and MVA LCD at the selected three primary colors ($R = 650$, $G = 550$, and $B = 450 \text{ nm}$), where the polarizer and analyzer pair has a maximum transmittance of 35%. The birefringence dispersion of the LC materials as described in (5) has been taken into consideration. For the IPS mode, the RGB primaries all reach their respective maximum transmittance at $V = 5.0 V_{\text{rms}}$, which is the full-bright gray

level G255. For the MVA mode, RGB primaries reach their respective maximum transmittance at different voltages: the blue light reaches its maximum at $V = 4 V_{\text{rms}}$ and red light at $\sim 7 V_{\text{rms}}$. In the simulation, we chose the green light maximum transmittance voltage at $V = 5.0 V_{\text{rms}}$ as the gray level G255 for the green and red primaries, and $V = 4 V_{\text{rms}}$ as the G255 for the blue primary of the MVA LCD.

B. Color Gamut of LCD Panels Under LED and CCFL Backlights

The color gamut of a display is referred to the range of colors that it can reproduce or distinguish. For a LCD device such as a monitor or a TV panel, its gamut can be plotted with the device's RGB primaries. This is one of the most common uses of the CIE diagram, especially for comparing the color gamut of the LCD devices.

Fig. 3 show the transmission spectra of the CCFL and LED backlight units and color filters. The CCFL-BLU we employed here is a commercial wide gamut one. The LED-BLU consists of a series of separate RGB LEDs, where the red LED (AlInGaP) has a peak wavelength at $R \sim 630$ nm and a full-width-half-maximum FWHM ~ 22 nm, the green LED (InGaN) has a peak wavelength at $G \sim 530$ nm and FWHM ~ 43 nm, and the blue LED (InGaN) has a peak wavelength at $B \sim 460$ nm and FWHM ~ 24 nm [2], [3]. The color filters have their average peak transmittance at $R \sim 650$ nm, $G \sim 550$ nm and $B \sim 450$ nm. It can be seen that the RGB peak wavelengths of LED-BLU match better with those of color filters, and its respective bandwidth is narrower and without side-lobes, as compared to that of CCFL-BLU.

In our simulation, the RGB primaries of the LCDs are mainly referred as the light transmittance of the backlight unit through the respective RGB color filters. Since LEDs can be switched on and off in a few nanoseconds, it has been demonstrated that the separate RGB LEDs can be switched respectively with the RGB image content to realize the color sequential display [2]. Under this case, the color filters are not needed and the optical efficiency of the device can be improved.

Fig. 4 is a plot of the RGB primaries through the MVA LCD panel using CCFL-BLU, LED-BLU with color filters or RGB LED without color filters. The color gamut defined by the RGB LED color points from LED-BLU with color filters in the color diagram is larger than that of the CCFL primaries and the National Television System Committee (NTSC) standard primaries. It means that it is possible to obtain a more than 100% NTSC color gamut by properly selecting the LED colors and the color filters. As for the primaries of the separate RGB LED without color filters, the color space can be further widened from 114.2% to 128.6% NTSC color gamut. The color gamut of a LCD device using the conventional CCFL-BLU is usually about 75% NTSC [22], [23]. Meanwhile, even though a wide gamut CCFL-BLU has been commonly adopted by LCD industry, the color gamut achieved by the CCFL backlight is 95.4% of the NTSC standard, which is still narrower than that of LED backlights. This is because the peak transmittance of the RGB primary colors of LED-BLU match better with those of color filters and their respective bandwidth is narrower.

Table I compares the color gamut of MVA and IPS LCDs under different backlights. It can be found that the color gamut

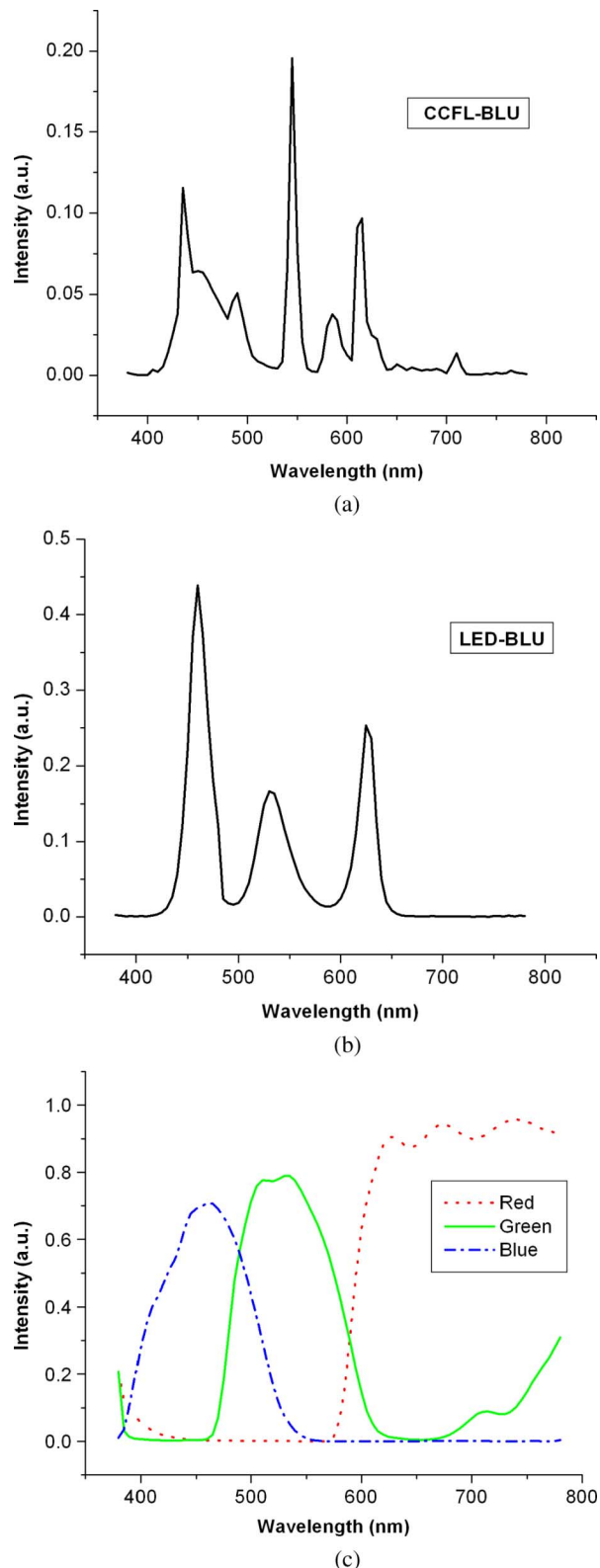


Fig. 3. Light source spectra of: (a) CCFL-BLU, (b) LED-BLU, and (c) CF transmittance spectra.

of IPS panel is 91.8%, 110.7% and 127.4% NTSC for the CCFL-BLU, LED-BLU with CFs, and LED-BLU without CFs, respectively. These data are all slightly lower than those of MVA LCD.

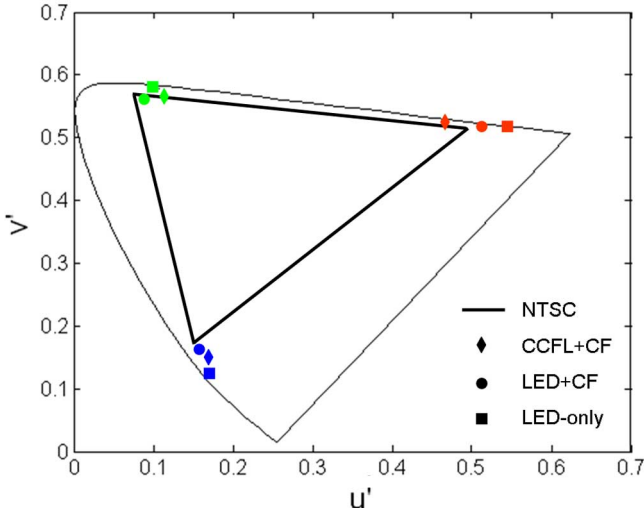


Fig. 4. RGB primaries through the film-compensated MVA-LCD panel for LED and CCFL backlights and NTSC standard primaries on the CIE 1976 UCS diagram.

TABLE I
SIMULATED COLOR GAMUT OF THE FILM-COMPENSATED IPS AND MVA LCDS AT THREE DIFFERENT BACKLIGHTS. (THE REFERENCED COLOR GAMUT OF NTSC STANDARD IS 1.0000)

	CCFL+CF	LED+CF	LED-only
MVA	0.9539	1.1416	1.2859
IPS	0.9177	1.1071	1.2737

C. Color Shift for RGB Primaries at Different Incident Angles

In this part, we further plot the CIE 1976 UCS diagrams with different incident angles at the full-bright gray level G255 for the IPS and MVA LCDs with different backlights. The incident angle is defined as the angle between the light incident direction and the normal of the LCD panel, which is referred as theta angle θ thereafter. In our calculations, we vary the theta angle from -80° to 80° , and scan the backlights across the whole 360° azimuthal angle (ϕ) at 10° scanning step for every chosen theta angle.

As shown in Fig. 5, the film-compensated MVA LCD exhibits a weaker color shift than the film-compensated IPS LCD in the RGB primaries with different backlights, especially in the blue primary. The separate RGB LED-BLU without CFs has an evidently much lower color shift than the CCFL-BLU and LED-BLU with CFs.

To quantitatively investigate angular color uniformity, we re-define (4) as

$$\Delta u'v' = \sqrt{(u'_{\max} - u'_{\min})^2 + (v'_{\max} - v'_{\min})^2} \quad (10)$$

where $[u'_{\max}, v'_{\max}]$ and $[u'_{\min}, v'_{\min}]$ represent the maximum and minimum $[u', v']$ values at the full-bright state between 0° – 80° viewing range. The data are summarized in Table II.

For the angular color shift of the film-compensated MVA and IPS LCDs under LED-BLU with CFs, we obtain $\Delta u'v' = (0.0110, 0.0274, 0.1101)$ for MVA LCD and

$\Delta u'v' = (0.0131, 0.0331, 0.1634)$ for IPS LCD at the RGB primaries. The MVA LCD has $\sim 20\%$ lower $\Delta u'v'$ values than IPS LCD, which implies the film-compensated MVA mode has better angular color uniformity than the film-compensated 4-domain IPS mode. Similar conclusions can be drawn when we compare the two LC modes using CCFL with CFs and RGB LED-BLU without CFs.

To compare the angular color uniformity of the film-compensated MVA LCD with different backlights, we obtain $\Delta u'v' = (0.0159, 0.0343, 0.1258)$ for CCFL-BLU with CFs, and $\Delta u'v' = (0.0083, 0.0254, 0.0511)$ for RGB LED-BLU without CFs at the respective RGB primaries. The LED backlit MVA-LCD shows $\sim 1.35X$ better angular color uniformity in green and $\sim 2X$ in red and blue primaries than the CCFL-based MVA-LCD. A similar trend is observed in the IPS LCD with different backlights.

To understand why the film-compensated MVA exhibits smaller color shift than the film-compensated multi-domain IPS, we look into the uncompensated device structures first. Fig. 6 shows the angular color uniformity of the MVA and IPS LCDs without any compensation films. For the CCFL BLU with color filters, the four-domain MVA LCD has $\Delta u'v' = (0.0200, 0.0555, 0.1968)$ at the RGB primaries while the four-domain IPS has $\Delta u'v' = (0.0148, 0.0471, 0.1801)$. For the LED BLU with color filters, the MVA has $\Delta u'v' = (0.0153, 0.0409, 0.1773)$ while IPS LCD has $\Delta u'v' = (0.0109, 0.0387, 0.1675)$ at the RGB primaries. From above results, the uncompensated IPS-LCD exhibits lower $\Delta u'v'$ values than the uncompensated MVA at the corresponding RGB primaries. It indicates that the uncompensated IPS LCD has better angular color uniformity than the uncompensated MVA LCD.

It has been shown that color shift can be suppressed in the multi-domain IPS LCD when observed at a fixed oblique viewing angle around the whole 360° azimuthal angle [24]. In this paper, we calculated the color shift based on the color difference between the oblique viewing angle and the normal viewing angle from (4). Therefore, the origin why the film-compensated MVA has a smaller angular color shift than the film-compensated IPS is primarily attributed to the optimized compensation films we employed. The LC alignment difference and the LC domain variation in the full-bright state only make secondary contributions. In a film-compensated MVA LCD, the compensation films are laminated on both sides of the LCD which can more effectively cancel the color dispersion from the uniaxial films themselves. In an IPS LCD, the films are only laminated on one side of the LCD. As a result, its color shift is more pronounced than that of MVA at large viewing angles.

D. Color Shift in the Horizontal Direction

In evaluating the color uniformity of a LCD monitor or TV, the observers care more about the color performance in the horizontal and vertical directions. Thus, the color shift in the horizontal direction is usually measured [22].

Fig. 7 shows the simulated angular dependent $\Delta u'v'$ of the LED- and CCFL-backlit MVA and IPS LCDs as observed from the horizontal ($\phi = 0^\circ$) viewing direction. For the IPS LCD backlit by CCFL- or LED-BLU with CFs (see Fig. 7(a)), the

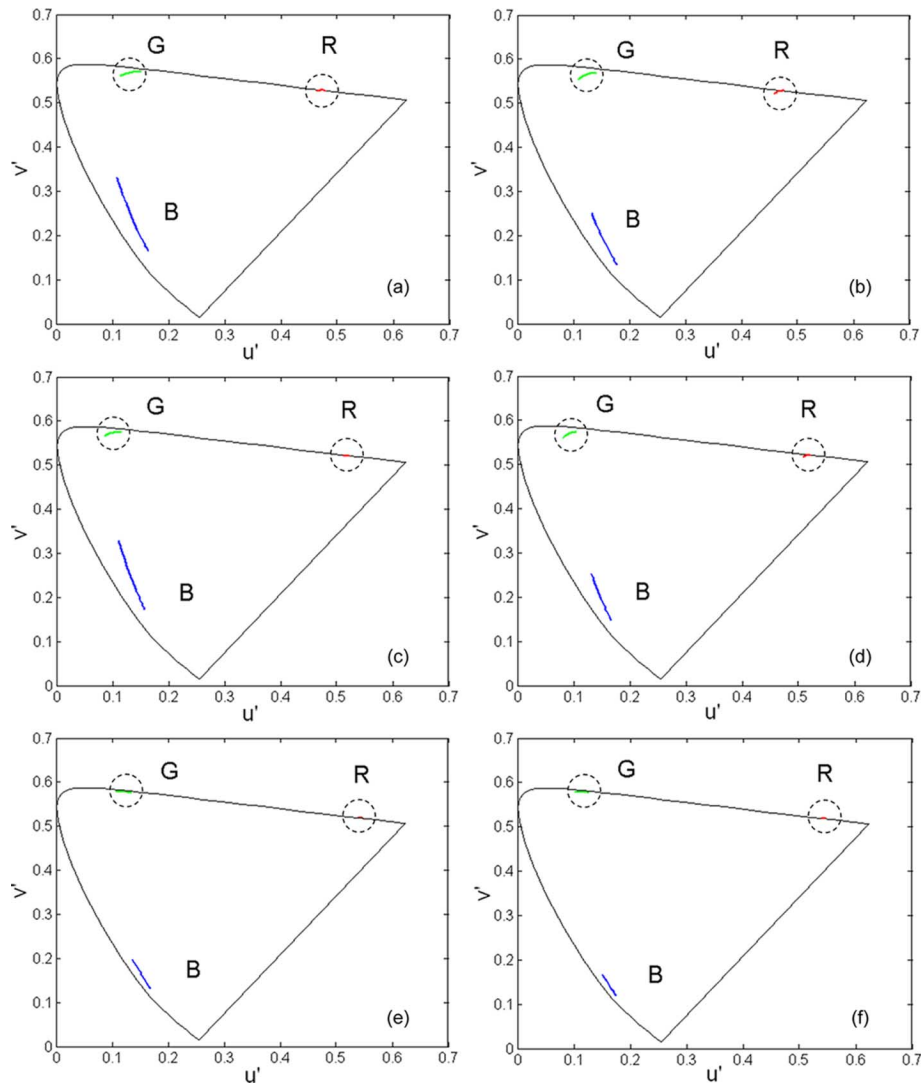


Fig. 5. Color shift for RGB primaries in the film-compensated LCDs as theta angle is varied from -80° to 80° : (a) IPS using CCFL-BLU with CFs; (b) MVA using CCFL-BLU with CFs; (c) IPS using LED-BLU with CFs; (d) MVA using LED-BLU with CFs; (e) IPS using LED-BLU without CFs; and (f) MVA using LED-BLU without CFs.

TABLE II

CALCULATED $\Delta u'v'$ VALUES OF THE FILM-COMPENSATED IPS AND MVA LCDS WITH THREE DIFFERENT BACKLIGHTS. THE THETA ANGLE IS VARIED FROM -80° TO 80° , AND EVERY THETA ANGLE IS SCANNED ACROSS THE WHOLE 360° AZIMUTHAL ANGLE (θ) AT 10° SCANNING STEP

		CCFL+CF	LED+CF	LED-only
MVA	R	0.0159	0.0110	0.0083
	G	0.0343	0.0274	0.0254
	B	0.1258	0.1101	0.0511
IPS	R	0.0183	0.0131	0.0089
	G	0.0392	0.0331	0.0304
	B	0.1755	0.1634	0.0725

RGB curves are fairly symmetric along the theta angle $\theta = 0^\circ$, where $\Delta u'v' = 0$ for different primaries. As the absolute value of theta angle increases, $\Delta u'v'$ gradually increases. In both LED- and CCFL-backlit IPS LCDs, blue color has the largest $\Delta u'v'$ value, followed by green and then red. Meanwhile, the

$\Delta u'v'$ value of LED backlit IPS LCD is smaller than that of the CCFL one for the respective RGB primaries when $|\theta| > 0$. At theta angle $\theta = -80^\circ$, $\Delta u'v' = (0.0103, 0.0292, 0.1320)$ for LED-BLU and $\Delta u'v' = (0.0148, 0.0351, 0.1422)$ for CCFL-BLU for the RGB primary, respectively.

Fig. 7(b) shows the similar plots for the MVA LCD backlit by CCFL- or LED-BLU with CFs. The RGB curves are still roughly symmetric along $\theta = 0^\circ$ and their values are lower than those of IPS LCD with the corresponding backlights. Similarly, the $\Delta u'v'$ value increases as the theta angle increases. In both LED and CCFL backlit MVA LCDs, blue color has the largest $\Delta u'v'$ value, and then followed by green and red. In the region that $|\theta| > 0$, the $\Delta u'v'$ of LED backlit MVA LCD is smaller than that of the CCFL-BLU for the respective RGB primaries. At $\theta = -80^\circ$, $\Delta u'v' = (0.0099, 0.0235, 0.1100)$ for LED-BLU and $\Delta u'v' = (0.0139, 0.0292, 0.1238)$ for CCFL-BLU at the respective RGB primaries. These values are all smaller than those of IPS LCD with the respective backlights. It demonstrates that LCDs using LED-BLU is helpful for reducing the color shift and the film-compensated MVA mode

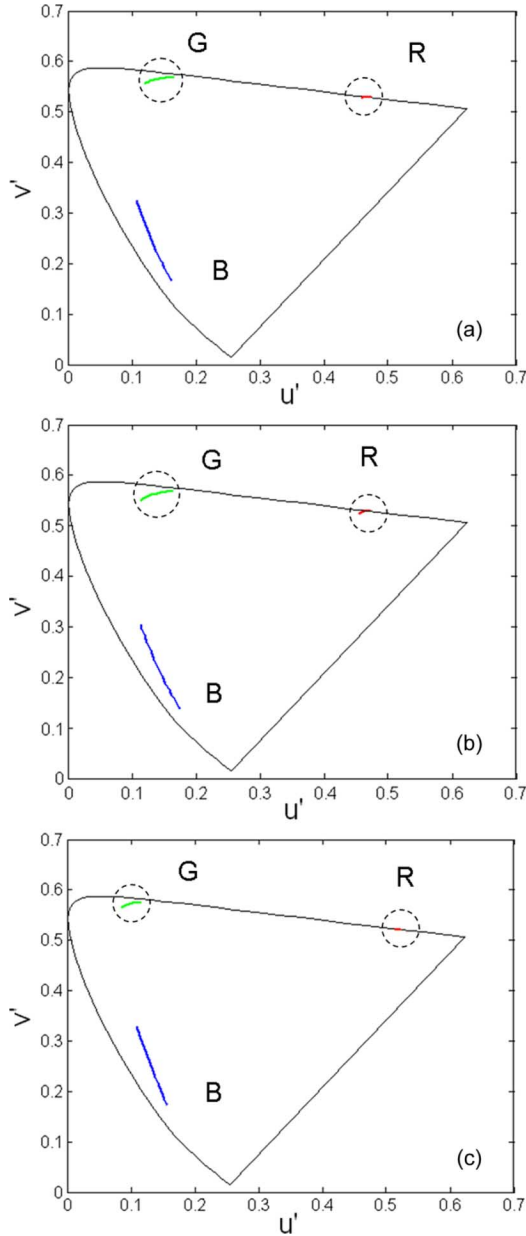


Fig. 6. Color shift of the uncompensated LCDs as theta angle increases from -80° to 80° . (a) IPS using CCFL-BLU with CFs. (b) MVA using CCFL-BLU with CFs. (c) IPS using LED-BLU with CFs. (d) MVA using LED-BLU with CFs.

has a slightly weaker color shift than the film-compensated IPS mode.

Fig. 7(c) compares the angular dependent $\Delta u'v'$ of the separate RGB LED-BLU without CFs for MVA and IPS LCDs. It can be seen that the RGB curves have been lowered quite a lot as compared to the LCDs backlit with CFs for both CCFL-BLU and LED-BLU. In the meantime, the $\Delta u'v'$ of the color-sequential RGB LED backlit MVA LCD is still smaller than that of the IPS mode at the RGB primaries. At $\theta = -80^\circ$, the $\Delta u'v'$ values for the RGB primaries are as low as (0.0073, 0.0222, 0.0431) for MVA LCD and (0.0083, 0.0270, 0.0569) for IPS LCD. The $\Delta u'v'$ values are ~ 1.3 – 2.5 X smaller than the conventional CCFL-BLU system. This advantage is attributed to the narrower spectral bandwidth and less overlap of the RGB LED light sources.

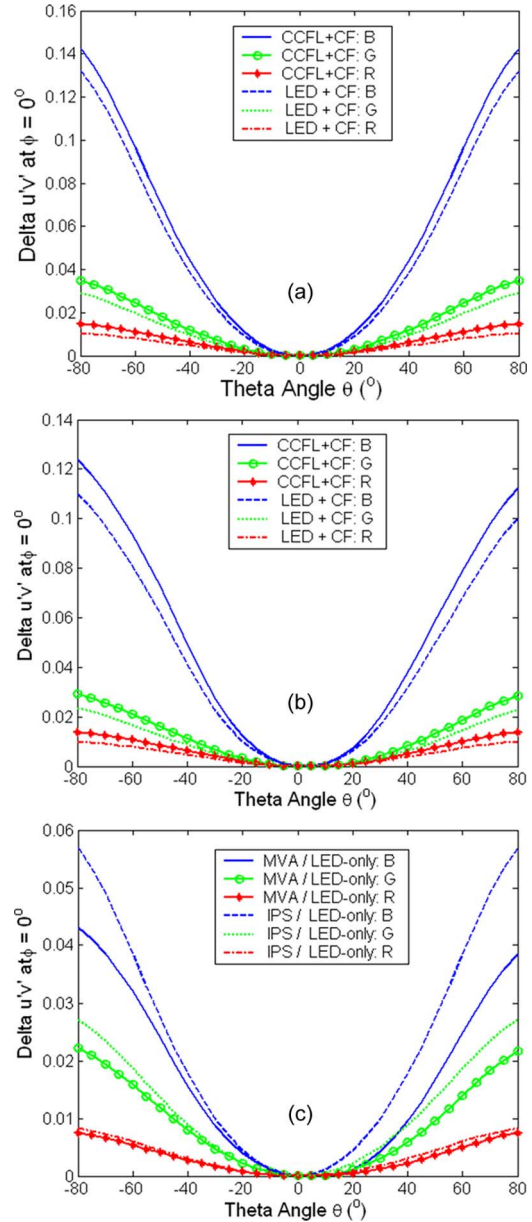


Fig. 7. Color shift for RGB primaries in the film-compensated LCDs under different backlights along the horizontal direction. (a) IPS using CCFL-BLU and LED-BLU with CFs. (b) MVA using CCFL-BLU and LED-BLU with CFs. (c) IPS and MVA using LED-BLU without CFs.

The color sequential LCD using RGB LEDs not only exhibits superior color performances, but also eliminate color filters and triples the device resolution. However, to achieve color-sequential the LC response time (gray to gray) should be faster than ~ 2 ms in order to avoid color breakup. To achieve fast response time, optically-compensated bend cell [25], thin cell gap, overdrive and undershoot voltage method, and elevated temperature operation have been investigated [17].

V. CONCLUSION

We have obtained quantitative results of the multi-domain IPS and MVA LCDs using RGB LEDs and CCFL as the backlight units. The LED backlit LCDs not only exhibits a wider color gamut but also has a ~ 1.3 – 2.5 X smaller color shift than that of CCFL-BLU especially when no color filters are used. In addi-

tion, the film-compensated MVA LCD generally has better angular color uniformity than the IPS mode under different backlights. Wide spread applications of LED backlights for high-end LCD monitors and LCD TVs are foreseeable.

REFERENCES

- [1] T. Otani, "LED backlights boost LCD TV color," *Nikkei Electron. Asia*, pp. 22–26, Mar. 2005.
- [2] G. Harbers and C. Hoelen, "High performance LCD backlight using high intensity red, green and blue light emitting diodes," in *Soc. Inf. Display Tech. Dig.*, 2001, vol. 32, pp. 702–705.
- [3] H. Hsieh, C. Chou, and W. Li, "Vivid color and clear motion picture 32-inch TFT-LCD TV with scan RGB LED backlight," in *Proc. Int. Display Manuf. Conf.*, 2005, pp. 622–644.
- [4] A. Konno, Y. Yamamoto, and T. Inuzuka, "RGB color control system for LED backlight in IPS-LCD TVs," in *Soc. Inf. Display Tech. Dig.*, May 2005, vol. 36, pp. 1380–1383.
- [5] W. Kim, "Technology overview: LCDs for TV application," *J. Soc. Inf. Display*, vol. 12, pp. 449–453, Dec. 2004.
- [6] J. Chen, K. Kim, J. Jyu, J. Souk, J. Kelly, and P. Bos, "Optimum film compensation modes for TN and VA LCDs," in *SID Symp. Dig.*, May 1998, vol. 29, pp. 315–318.
- [7] D. Kajita, I. Hiyama, U. Utsumi, M. Ishii, and K. Ono, "Wide-viewing angle IPS-LCD for TV applications using optical compensation technology," *Proc. SPIE*, vol. 6135, pp. 613502-1–613502-10, 2006.
- [8] R. Lu, X. Zhu, S. T. Wu, Q. Hong, and T. X. Wu, "Ultrawide-view liquid crystal displays," *J. Display Technol.*, vol. 1, pp. 3–14, Sept. 2005.
- [9] M. Fairchild, *Color Appearance Models*, 2nd ed. Hoboken, NJ: Wiley, 2005.
- [10] F. Bunting, *Color Primer—An Introduction to the History of Color, Color Theory, and Color Measurement*. Larkspur, CA: Light Source Computer Images, Inc., 1998.
- [11] N. Ohta and A. Robertson, *Colorimetry—Fundamentals and Applications*. Hoboken, NJ: Wiley, 2005.
- [12] G. Wyszecki and W. Stiles, *Color Science—Concepts and Methods, Quantitative Data and Formulate*, 2nd ed. New York: Wiley, 1982.
- [13] R. Hunt, *Measuring Colour*, 2nd ed. West Sussex, U.K.: Ellis Horwood, 1991.
- [14] R. Lu, S. T. Wu, Z. Ge, Q. Hong, and T. X. Wu, "Bending angle effects on the multi-domain in-plane-switching liquid crystal displays," *J. Display Technol.*, vol. 1, no. 2, pp. 207–216, Dec. 2005.
- [15] S. Kim, "Super PVA sets new state-of-the-art for LCD-TV," in *SID Symp. Dig.*, May 2004, vol. 35, pp. 760–763.
- [16] S. T. Wu, "Birefringence dispersion of liquid crystals," *Phys. Rev. A*, vol. 33, pp. 1270–1274, Feb. 1986.
- [17] S. T. Wu and D. K. Yang, *Reflective Liquid Crystal Displays*. Hoboken, NJ: Wiley, 2001.
- [18] Q. Hong, T. X. Wu, X. Zhu, R. Lu, and S. T. Wu, "Extraordinary high-contrast and wide-view liquid crystal displays," *Appl. Phys. Lett.*, vol. 86, p. 121107, Mar. 2005.
- [19] R. Lu, Q. Hong, and S. T. Wu, "Characteristics of a twelve-domain MVA-LCD," *J. Display Technol.*, vol. 2, no. 3, pp. 217–222, Sep. 2006.
- [20] S. T. Wu, "Phase-matched compensation films for liquid crystal displays," *Materials Chemistry and Physics*, vol. 42, pp. 163–168, 1995.
- [21] A. Lien, "A detailed derivation of extended Jones matrix representation for twisted nematic liquid crystal displays," *Liq. Cryst.*, vol. 22, pp. 171–175, Feb. 1997.
- [22] M. Hsieh, K. Peng, Y. Hsu, M. Shih, H. Hung, C. Hung, H. Hsieh, W. Li, M. Yang, and C. Wei, "Recent improvements of multidomain-vertically-aligned-mode LCD TV," in *SID Symp. Dig.*, Jun. 2006, vol. 37, pp. 1942–1945.
- [23] R. Lu, Q. Hong, Z. Ge, and S. T. Wu, "Color shift reductions of a multi-domain IPS-LCD using RGB-LED backlight," *Opt. Expr.*, vol. 14, pp. 6243–6252, June 2006.
- [24] H. Klausmann, S. Aratani, and K. Kondo, "Optical characterization of the in-plane switching effect utilizing multidomain structures," *J. Appl. Phys.*, vol. 83, pp. 1854–1862, Feb. 1998.
- [25] C. Pan, S. Jeng, C. Wu, and P. Hsu, "A 32-in. high-contrast-ratio OCB (Optical Compensation Bend) LCD TV," in *SID Symp. Dig.*, Jun. 2006, vol. 37, pp. 1344–1345.



Ruibo Lu received the Ph.D. degree in optics from Department of Physics, Fudan University, Shanghai, China, in 1998, and M.S. degree in applied physics from Department of Physics, East China University of Science and Technology, Shanghai, China, in 1995. His research work in Ph.D. focused on liquid crystal alignment and ferroelectric liquid crystal devices for display and advanced optical applications. He was a faculty in Department of Physics, and later in Department of Optical Science and Engineering, Fudan University, China, from 1998 to 2001. He was an optical engineer in Lightwaves2020 Inc., San Jose, CA, from 2001 to 2002. Since then, he joined the School of Optics/CREOL (now as College of Optics and Photonics), University of Central Florida, Orlando, as a research scientist. His research interests include liquid crystal display technology, wide viewing angle for liquid crystal TVs, liquid crystal components for optical communications and optical imaging using liquid crystal medium.



Qi Hong received B.S. degree from the Nanjing University of Aeronautics and Astronautics, Nanjing, China, in 1992, and the M.S.E.E. degree from the University of Central Florida, Orlando, in 2002, where he is currently pursuing the Ph.D. degree in the electrical engineering.

He was a Design Engineer at the Xiaxin Electronics Company Ltd., Xiamen, China, from 1992 to 2000. His doctoral research topics include liquid crystal device modeling, wide viewing angle and fast response liquid crystal display.



Shin-Tson Wu (M'98–SM'99–F'04) received the B.S. degree in physics from National Taiwan University, and the Ph.D. degree from the University of Southern California, Los Angeles.

He is a PREP professor at College of Optics and Photonics, University of Central Florida (UCF). His studies at UCF concentrate in foveated imaging, bio-photonics, optical communications, liquid crystal displays, and liquid crystal materials. Prior to joining UCF in 2001, he worked at Hughes Research Laboratories, Malibu, CA, for 18 years.

He has co-authored 4 books: *Fundamentals of Liquid Crystal Devices* (Wiley, 2006, with D. K. Yang); *Introduction to Microdisplays* (Wiley, 2006, with D. Armitage and I. Underwood) *Reflective Liquid Crystal Displays* (Wiley, 2001, with D. K. Yang) and *Optics and Nonlinear Optics of Liquid Crystals* (World Scientific, 1993, with L. C. Khoo), 5 book chapters, and over 350 journal papers. He has more than 55 issued and pending patents. Several of his patents have been implemented in display and photonic devices.

Dr. Wu is a Fellow of the Society of Information Display (SID) and Optical Society of America (OSA).

Kuo-Hsuan Peng, photograph and biography not available at time of publication.

Hung-Sheng Hsieh, photograph and biography not available at time of publication.